




Synthesis of As-Cast WCu Composite Containing Micro- and Nano-Size Tungsten Particles Using Aluminothermic Reduction

CHU CHENG ^{1,2,3,5}, KE-XING SONG^{1,2,3}, ZI-WEI SONG¹,
LING-FENG WANG¹, QIAN-QIAN XU¹, LING-LIANG ZHANG¹,
CHAO HAN¹, ZHI-HE DOU⁴, and TING-AN ZHANG⁴

1.—School of Materials Science and Engineering, Henan University of Science and Technology, Luoyang 471023, China. 2.—Provincial and Ministerial Co-construction Collaborative Innovation Center of Nonferrous New Materials and Advanced Processing Technology, Luoyang 471023, China. 3.—Henan Key Laboratory of Non-ferrous Materials Science and Processing Technology, Luoyang 471023, China. 4.—Key Laboratory of Ecological Metallurgy of Multi-metal Intergrown Ores of Ministry of Education, School of Metallurgy, Northeastern University, NO. 3-11, Wenhua Road, Heping District, Shenyang 110819, People's Republic of China. 5.—e-mail: cheng_chu_love@126.com

Herein, we present a novel methodology for preparing an as-cast WCu composite ingot, containing micro- and nano-size tungsten particles, through aluminothermic reduction. To synthesize the WCu composite ingot, the thermodynamics and dynamics of the Al-CuO-WO₃ and Al-CuO-WO₃-CaO system were investigated; thereafter, the WCu composite ingot and slag obtained through the aluminothermic reduction were systematically analyzed. The results indicate that the aluminothermic reduction occurs within a temperature range of 1223–1233 K, and the addition of CaO decreases the exothermic intensity and delays the aluminothermic reduction reaction time. The microstructure of the WCu ingot comprises a gray matrix, white tungsten particles, and black inclusions; moreover, the tungsten particle size ranges from 1 μm to 10 μm, with an average diameter of 3.52 μm and average area of 13.85 μm². The slag mainly comprises CaAl₄O₇, CaWO₄, and Al₂O₃.

INTRODUCTION

WCu is widely used in applications, such as electrical contacts for high-voltage switches, resistance welding electrodes, and aerospace rocket nozzles, owing to its high density, high strength, hardness, good electrical and thermal conductivity, and arc erosion resistance.^{1–3} Because tungsten and copper are immiscible, WCu is a typical pseudo-alloy, which is conventionally considered a composite material.⁴ However, fabricating WCu through direct smelting is difficult because of the distinct differences in the melting point and the insolubility between W and Cu.⁵ Currently, WCu is fabricated through the infiltration technique and high-

temperature sintering method based on powder metallurgy using superfine metal powders as raw materials.^{6,7} Notably, the high sintering temperature, long fabrication time, and low density obtained from typical fabrication methods result in high cost, high-energy consumption, low productivity, and, most importantly, poor product performance.⁸

Researchers worldwide have focused on improving the microstructure uniformity and density of WCu by preparing micro- or nano-size WCu composite particles using powder metallurgy. Chen⁹ demonstrated that the relative density of WCu increased with a decrease in the particle size of tungsten and copper powders. When the particle size decreased from 20.69 μm to 0.52 μm, its relative density increased from 97.5% to 99.2%. Gong and Li^{10,11} prepared an ultrafine nano-WCu composite with a tungsten grain size of approximately 2 μm and density > 99.0% through high-performance ball

(Received July 21, 2021; accepted November 13, 2021;
published online January 6, 2022)

milling, followed by sintering. Lee and Wang^{12,13} separately prepared micro- or nano-size WCu composite particles using chemical processes, such as the mechanical-thermochemical, chemical coprecipitation, and sol-gel methods. The obtained WCu composite particles were then sintered; the WCu composite was produced with a uniform microstructure, grain size $< 1 \mu\text{m}$ and density of approximately 99.2–99.7%. In conclusion, the above methods can effectively improve the density and refine the grain structure of WCu by reducing the particle size of the raw materials. However, these techniques increase the complexity associated with the preparation process of micro-nano WCu composite powder, which, in turn, increases the complexity associated with the production process of WCu composites. In addition, methods based on powder metallurgy rely on the high-temperature sintering process of powder metallurgy, which possess disadvantages such as high-energy consumption and low-production efficiency that are difficult to overcome. In this study, to overcome the disadvantages of powder metallurgy, a novel method of synthesizing as-cast WCu composite ingot containing micro- and nano-size tungsten particles using aluminothermic reduction is presented. WO_3 , CuO, and Al powders were used as the raw materials to induce a self-propagation high-temperature synthesis (SHS) reaction, which resulted in synthesizing a high-temperature WCu composite melt containing in situ micro- and nano-size tungsten particles. To produce low-melting-point calcium aluminates, CaO, which is used as forming slag, was combined with the generated Al_2O_3 . After the SHS reaction, the metal and slag were phase separated owing to differences in density; finally, an as-cast WCu composite ingot, containing micro- and nano-size tungsten particles, was obtained. Compared to powder metallurgy, first, micro- and nano-size tungsten particles were synthesized in situ, which is beneficial to their homogeneous distribution and interface bonding. Second, the as-cast ingot synthesized by aluminothermic reduction was denser than an ingot obtained using powder metallurgy. In addition, this method has advantages of low-energy consumption and high-production efficiency. In this study, the thermodynamics and dynamics of the Al-CuO- WO_3 and Al-CuO- WO_3 -CaO system were investigated, and the WCu composite ingot and slag obtained after the aluminothermic reduction were systematically analyzed. We believe that this study will provide a theoretical basis for the efficient preparation of homogeneous and high-density WCu composites.

EXPERIMENTAL

Materials

WO_3 (99.90 wt.%, particle size: 80–100 nm) and CuO (99.50 wt.%, particle size: $\leq 0.20 \mu\text{m}$) were used as the raw materials. CaO (99.50% wt.%,

particle diameter: $\leq 0.25 \mu\text{m}$) and magnesium powder (99.50% wt.%, particle diameter: $\leq 0.2 \mu\text{m}$) were separately used as slagging agent and ignition agent, and they were obtained from Sinopharm Chemical Reagent Co., Ltd., China. Aluminum powder (99.5% pure, particle diameter: 0.1–3 mm) from Jinzhou Metal Co., Ltd., China, was used as a reductant.

Experimental Methods

WCu composite was synthesized under atmospheric pressure. To prepare the raw materials before synthesis, WO_3 , CuO, and CaO were heated in air at 523 K for 12 h to remove water. The mass percentages of WO_3 , CuO, CaO, and Al powder were 46.65 %, 30.87%, 4.63 %, and 17.85 %, respectively. The raw materials and Al powder were weighed and placed in a ball mill, in which alumina balls were added for ball-milling. The tank was covered with a lid, and the reagents were mixed for 40 min. The ingredients were preheated in an oven at 353 K for 20 min to supply extra heat for the reaction system, and then they were placed into a conical graphite reactor with a volume of 10 L, enclosed by a magnesia lining. Next, approximately 2–3 g of Mg powder was placed on top of the other reagents and ignited to induce the SHS and obtain a metal-slag mixed melt. CuO and WO_3 were reduced by Al powder, and the WCu composite melt containing in situ micro- and nano-size tungsten particles and Al_2O_3 was generated during the SHS. Al_2O_3 combined with CaO produced low-melting-point calcium aluminates. Thereafter, the melt was cast into a graphite crucible and cooled to approximately 298 K. Finally, the WCu composite ingot was obtained after removing the slag.

Calculation and Analysis Methods

The standard Gibbs free energy change (ΔG) of the possible reactions in the Al-CuO- WO_3 -CaO system was calculated under standard atmospheric pressure using HSC 6.0 software. A thermal analyzer (STA6000, PE Instruments, USA) was used to determine the change in heat flow of the Al-CuO- WO_3 and Al-CuO- WO_3 -CaO mixtures. Differential thermal analysis (DTA) was performed by heating the samples up to 1473 K at a heating rate of 10 K/min under an argon gas flow. The exothermic peaks of DSC curves were dealt with the Freeman–Carroll method, by which its apparent activation energy (E) and reaction order (n) were obtained. The samples of WCu composite ingot and slag were characterized using scanning electron microscopy (SEM) coupled with energy-dispersive x-ray spectroscopy (EDS) (SU-8010, Hitachi, Japan), and the phases of slags obtained through aluminothermic reduction were characterized using x-ray diffractometry (XRD) (Model D8, Bruker, Germany) with a Cu K α 1 source at 40 kV and 40 mA.

RESULTS AND DISCUSSION

Thermodynamics and Dynamics Analysis

Thermodynamics

Figure 1 shows the ΔG of the possible reactions in the Al-CuO-WO₃-CaO system. The result shows that the cupric and tungsten oxides with varying valence states can be reduced using Al, indicating that it is theoretically feasible to prepare a WCu composite through aluminothermic reduction. The ΔG of the reactions between CuO or CaO and WO₃, which generate CuWO₄ and CaWO₄, respectively, gradually increases from negative to positive with increasing temperature, and the value reaches zero at 753 K and 1573 K, respectively. This indicates that CuO and CaO can react with WO₃ to generate their respective products when the temperature is < 753 K and 1573 K, respectively. In contrast, these two reactions cannot proceed when the temperature is > 753 K and 1573 K, respectively. Therefore, it can be concluded that a higher temperature prevents the generation of CuWO₄ and CaWO₄, which is conducive to improving metal recovery methods.

DTA Analysis

Figure 2 shows the DTA curves of the Al-CuO-WO₃ and Al-CuO-WO₃-CaO systems. The results show that there is an endothermic peak (P_0) at 933 K in both the Al-CuO-WO₃ and Al-CuO-WO₃-CaO systems, where the Al powder melts. In the Al-CuO-WO₃ system, there are exothermic peaks (P_1 and P_2)

at 1153 and 1223 K, respectively. P_1 is reported to be an exothermic peak that arises from CuO reacting with WO₃ to produce CuWO₄.¹⁴ P_2 is a superimposed exothermic peak, where CuO and CuWO₄ are reduced by Al, and its E_2 and n_2 are calculated as 1039.31 kJ/mol and 3.16, suggesting that it is controlled by an intense chemical reaction. In the Al-CuO-WO₃-CaO system, there are exothermic peaks (P_3 , P_4 , and P_5) at 1123, 1173, and 1233 K, respectively. P_3 and P_4 are two exothermic peaks,

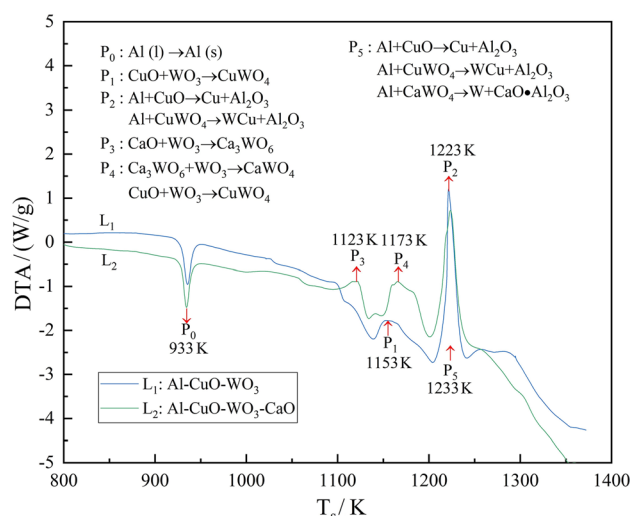


Fig. 2. DTA curves of the Al-CuO-WO₃ and Al-CuO-WO₃-CaO system.

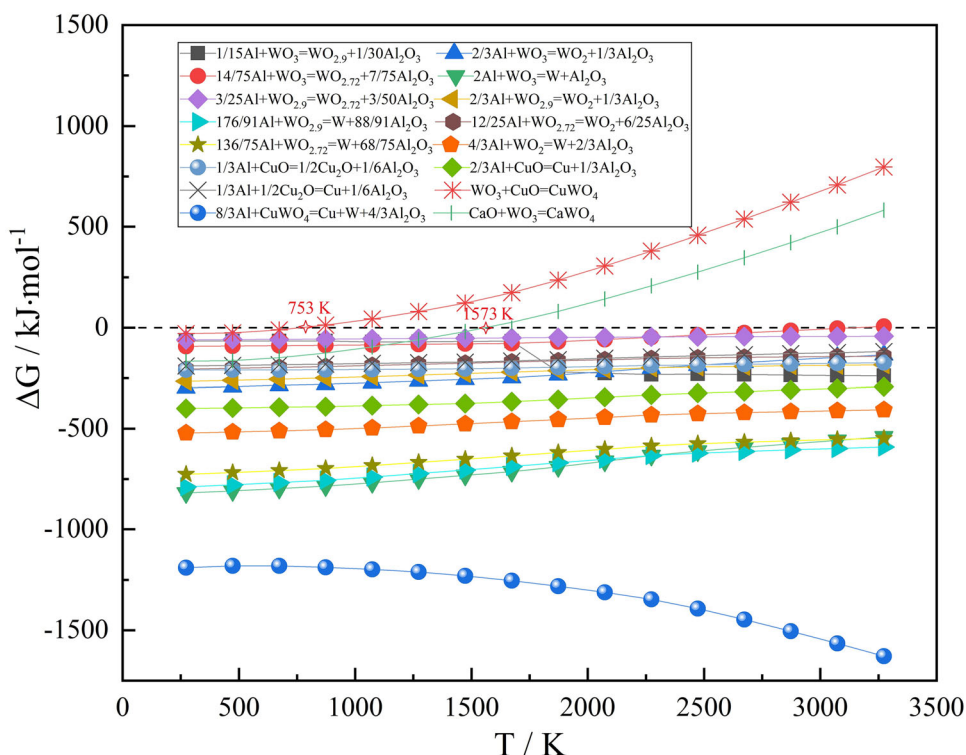


Fig. 1. ΔG of the possible reactions in the Al-CuO-WO₃-CaO system.

which result from CaO reacting with WO_3 to produce Ca_3WO_6 and the subsequent reaction between Ca_3WO_6 and WO_3 to produce CaWO_4 .¹⁵ In addition, a reaction between CuO and WO_3 to produce CuWO_4 may occur at P_4 . In accordance with the ratio of raw materials, P_5 is considered a superimposed exothermic peak, where CuO, CaWO_4 , and CuWO_4 are reduced by Al, and its E_5 and n_5 are calculated as 704.61 kJ/mol and 2.23, suggesting that it is also controlled by an intense chemical reaction. Upon comparing L_1 and L_2 , we noted that the exothermic peak, E_2 and n_2 of the aluminothermic reduction reaction in the Al-CuO- WO_3 system are sharper and higher, respectively, than those of the Al-CuO- WO_3 -CaO system. This indicates that the exothermic intensity of the Al-CuO- WO_3 system is reduced and that the aluminothermic reduction reaction is delayed owing to the addition of CaO.¹⁶

Characterizations of the WCu Composite Ingot

Figure 3 shows the characterization of the WCu composite ingot synthesized using aluminothermic reduction. Figure 3a shows that the microstructure of the WCu ingot primarily comprises gray matrix, white tungsten particles, and black inclusions. Figure 3b shows that the phase area percentages of the copper matrix, tungsten particles, and black inclusions are 58.36%, 39.95%, and 1.69%, respectively. As shown in Fig. 3c, a statistical analysis of the tungsten particle size distribution reveals that the tungsten particle size ranges from 1 μm to 10 μm , with an average diameter of 3.52 μm and average area of 13.85 μm^2 . Figure 3d, an enlargement of Area 1 in Fig. 3a, shows that the long strip structures are distributed on the smooth matrix, the spherical or ellipsoidal tungsten particles are evenly distributed on the matrix, and the black spherical inclusions are embedded between the tungsten particles and matrix. The element distribution (Fig. 3e–h) shows that Cu is evenly distributed on the matrix, W is distributed on the spherical or ellipsoidal tungsten particles, Al is mainly distributed on the matrix and black spherical inclusions, and O is only distributed on the black spherical inclusions. Figure 3i depicts the line scan diagram of L_1 in Fig. 3d, where the distribution of each element in the microstructure of WCu is consistent with the above surface scan results. Figure 3k–m shows the EDS analysis results of P_1 , P_2 , and P_3 in Fig. 3d, respectively. The EDS results show that the smooth matrix and long strip structures are both a Cu-Al solid solution;¹⁷ however, the content of Al in the long strip structures is slightly higher than that in the smooth matrix. The black spherical inclusion comprises Al and O. The atomic ratio of Al and O is close to 2:3, indicating that the inclusion is Al_2O_3 . Figure 3j, an enlargement of Area 2 in Fig. 3d, shows that a small amount of the

spherical black phase is discretely distributed on the white spherical or ellipsoidal tungsten particles. The EDS analysis results in Fig. 3n and o show that the spherical black phase comprises Cu, W, and Al, while the other part on the tungsten particle is only W. In addition, the smaller tungsten particles are bonded to the larger tungsten particles. It is speculated that the grain agglomeration and growth occurred during the formation of the large tungsten particles. Therefore, the size and morphology of the tungsten particles can be controlled by adjusting the parameters of the aluminothermic reduction.

Characterizations of the Slag

Figure 4 shows the XRD patterns of the slag obtained after thermite reduction. The diffraction peaks of CaAl_4O_7 , CaWO_4 , and Al_2O_3 appear in these XRD patterns, indicating that the main phases in the slag are CaAl_4O_7 , CaWO_4 , and Al_2O_3 . The thermodynamic calculation in Fig. 1 shows that CaO can react with WO_3 to produce CaWO_4 when the temperature is < 1573 K. Therefore, it can be inferred that CaWO_4 in the slag is a by-product that is formed while the temperature is rising during the aluminothermic reduction.

Figure 5 shows the microstructure, element distribution, and EDS analysis results of the slag obtained after the aluminothermic reduction. Figure 5a shows that the microstructure of the slag mainly comprises a white granular phase (P_1), gray strip phase (P_2), and matrix (P_3). The element distribution in Fig. 5b–f shows that Al and O are mainly distributed in the matrix (P_3) and gray strip phase (P_2), while the gray strip phase contains more Al and O than does the matrix. Ca is mainly distributed in the white granular phase (P_1) and matrix (P_3), whereas W is only distributed in the white granular phase (P_1). Figure 5g–i shows the EDS analysis results of the white granular phase (P_1), gray strip phase (P_2), and matrix (P_3). The atomic ratio of Ca, W, and O in the white particle phase (P_1) is close to 1:1:4, implying that the white particle is CaWO_4 . The atomic ratio of Al and O in the gray strip phase (P_2) is close to 2:3, indicating that the gray strip phase is Al_2O_3 . The atomic ratio of Ca, Al, and O in the matrix (P_3) is close to 1:4:7, indicating that the matrix is CaAl_4O_7 . In conclusion, the slag obtained after the aluminothermic reduction mainly comprises white CaWO_4 particles, and the gray strip comprises Al_2O_3 and CaAl_4O_7 . The analysis results are consistent with the XRD analysis of the slag in Fig. 4.

CONCLUSION

Herein, we prepared a WCu composite using aluminothermic reduction. A higher temperature was beneficial for preventing the generation of CuWO_4 and CaWO_4 . Al powder melted at 933 K in both the Al-CuO- WO_3 and Al-CuO- WO_3 -CaO systems. The aluminothermic reduction occurred

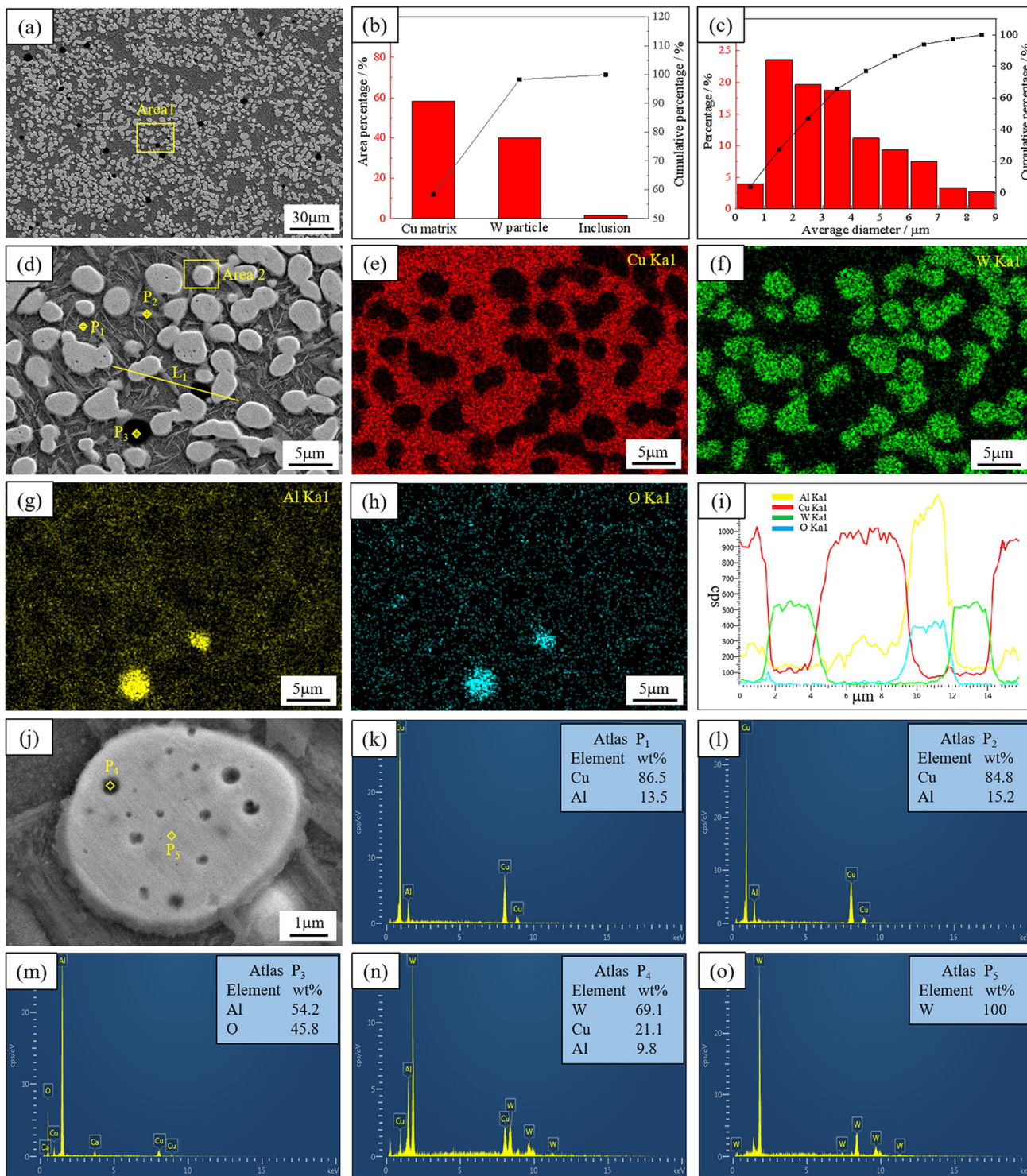


Fig. 3. Characterizations of the WCu composite ingot: (a–c) SEM image and phases analysis; (d–i) element distribution; and (j–o) EDS analysis results.

within a temperature range of 1223–1233 K, and the addition of CaO resulted in the decrease of the exothermic intensity and the delay of the aluminothermic reduction reaction time. The microstructure of the WCu ingot, which was

prepared using aluminothermic reduction, mainly comprised a gray matrix, white tungsten particles, and black Al_2O_3 inclusions, with phase area percentages of 58.36%, 39.95%, and 1.69%, respectively. The tungsten particle size ranged from 1 μm

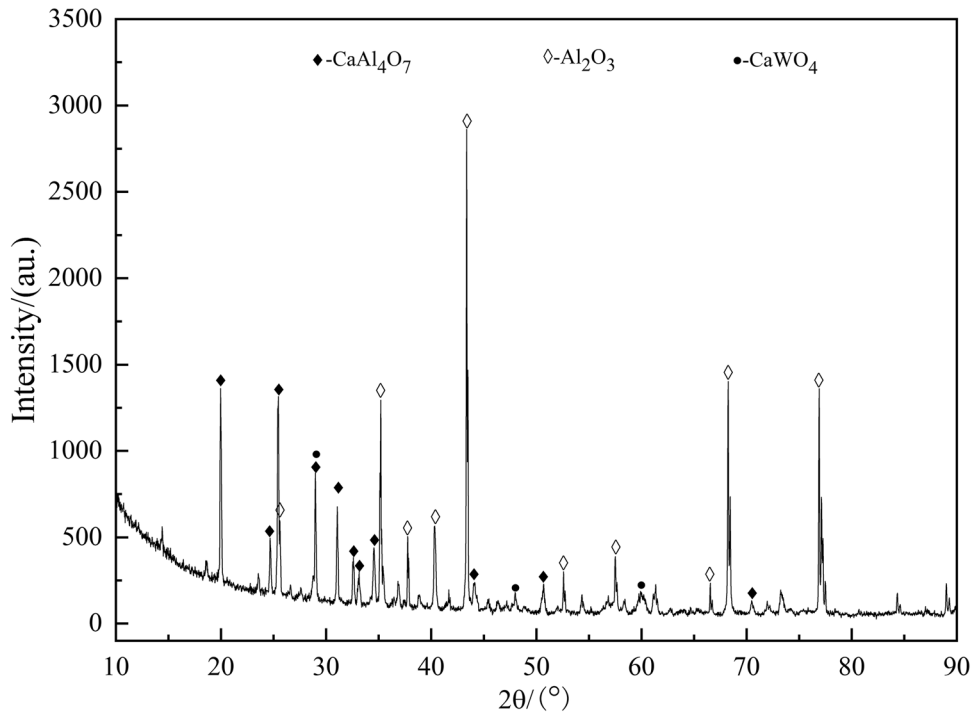


Fig. 4. XRD patterns of the slag obtained after aluminothermic reduction.

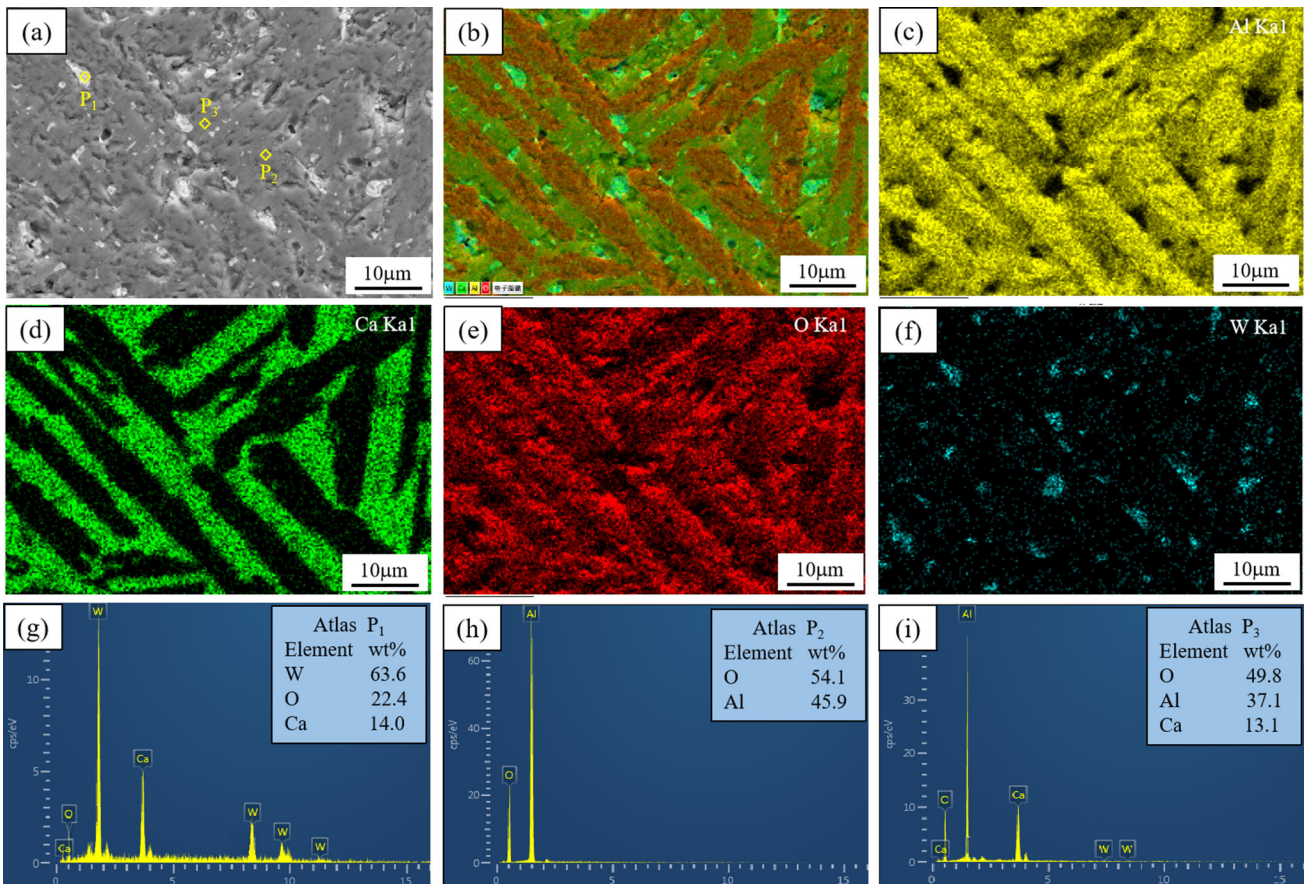


Fig. 5. Observation of the slag obtained after aluminothermic reduction: (a–f) element distribution and (g–i) EDS analysis results.

to 10 μm , with an average diameter of 3.52 μm and average area of 13.85 μm^2 . The slag obtained after the thermite reduction mainly comprised CaAl_4O_7 , CaWO_4 , and Al_2O_3 . CaWO_4 was formed as a by-product in the temperature-rise period during the aluminothermic reduction, and its formation decreased the yield of tungsten. The process for eliminating Al_2O_3 inclusions of the as-cast WCu composite will be the subject of subsequent papers.

CONFLICT OF INTEREST

The authors declare that they have no conflict of interest.

ACKNOWLEDGEMENTS

This research was supported by the Key Technologies R & D Program of Henan Province (Grant No. 202102210207), Chinese Postdoctoral Science Foundation (Grant No. 2020M672222), Doctoral Scientific Research Foundation of Henan University of Science and Technology (Grant No. 13480091), and Postdoctoral Scientific Research Foundation of Henan University of Science and Technology (Grant No. 13554020).

REFERENCES

1. Q. Zhang, S. Liang, and L. Zhuo, *J. Alloys Compd.* 708, 796. (2017).
2. J. Zou, D. Song, H. Shi, and S. Liang, *Mater. Res. Express* 7(2), 26528. (2020).

3. Y.L. Wang, S.H. Liang, and N. Luo, *Rare Met. Mater. Eng.* 45(2), 329. (2016).
4. Q. Zhang, S. Liang, and L. Zhuo, *Mater. Sci. Technol.* 33(17), 2071. (2017).
5. Y. Guo, H. Guo, B. Gao, X. Wang, Y. Hu, and Z. Shi, *J. Alloys Compd.* 724, 155. (2017).
6. G. He, P. Zhao, S. Guo, Y. Chen, G. Liu, and J. Li, *J. Alloys Compd.* 579, 71. (2013).
7. C. Wang, S. Liang, F. Cao, and Q. Zhang, *J. Alloys Compd.* 816, 152506. (2019).
8. L. Zhuo, Q. Zhang, Y. Zhang, Z. Zhao, and J. Zhang, *J. Nucl. Mater.* 538, 152220. (2020).
9. W. Chen, L. Dong, Z. Zhang, and H. Gao, *J. Mater. Sci. Mater. Electron.* 27(6), 5584. (2016).
10. C.P. Liang, C.Y. Wu, J.L. Fan, and H.R. Gong, *J. Phys. Chem. Solids* 34(6), 401. (2017).
11. Y.P. Li, X.H. Qu, and Z.H. Zheng, *Int. J. Refract. Met. Hard Mater.* 5(6), 259. (2003).
12. G.G. Lee, G.H. Ha, and B.K. Kim, *Powder Metall.* 43(1), 79. (2000).
13. X.R. Wang, S.Z. Wei, L.J. Xu, J.W. Li, and X.Q. Shan, *Adv. Powder Technol.* 29(6), 1323. (2018).
14. E.X. Wu, C.L. Qian, Z.Q. Zou, and Y.H. Zhang, *J. Cent.-South Inst. Min. Metall.* 24(1), 64. (1993).
15. G. Flor, V. Massarotti, and R. Riccardi, *Zeitschrift für Naturforschung a* 32(2), 160. (1977).
16. C. Cheng, Z.H. Dou, T.A. Zhang, H.J. Zhang and J. M: JOM, 69(2), 1818 (2017).
17. Z.R. Tang, and R.Z. Tian, *Binary Alloy Phase Diagrams and Crystal Structure of Intermediate Phase* (Central South University Press, Changsha, 2009), p. 51.

Publisher's Note Springer Nature remains neutral with regard to jurisdictional claims in published maps and institutional affiliations.